
Guiding Deep Molecular Optimization with Genetic Exploration

Sungsoo Ahn Junsu Kim Hankook Lee Jinwoo Shin

Korea Advanced Institute of Science and Technology (KAIST)

{sungsoo.ahn, junsu.kim, hankook.lee, jinwoos}@kaist.ac.kr

Abstract

De novo molecular design attempts to search over the chemical space for molecules with the desired property. Recently, deep learning has gained considerable attention as a promising approach to solve the problem. In this paper, we propose genetic expert-guided learning (GEG), a simple yet novel framework for training a deep neural network (DNN) to generate highly-rewarding molecules. Our main idea is to design a “genetic expert improvement” procedure, which generates high-quality targets for imitation learning of the DNN. Extensive experiments show that GEG significantly improves over state-of-the-art methods. For example, GEG manages to solve the penalized octanol-water partition coefficient optimization with a score of 31.82, while the best-known score in the literature is 26.1. Besides, for the GuacaMol benchmark with 20 tasks, our method achieves the highest score for 19 tasks, in comparison with state-of-the-art methods, and newly obtains the perfect score for three tasks.

1 Introduction

Discovering new molecules with the desired property is fundamental in chemistry, with critical applications such as drug discovery [1] and material design [2]. The task is challenging since the molecular space is vast; e.g., the number of synthesizable drug-like compounds is estimated to be around 10^{60} [3]. To tackle this problem, *de novo molecular design* [4, 5] aims to generate a new molecule from scratch with the desired property, rather than naïvely enumerate over the molecular space.

Over the past few years, molecule-generating deep neural networks (DNNs) have demonstrated successful results for solving the de novo molecular design problem [6, 7, 8, 9, 10, 11, 12, 13, 14, 15, 16, 17, 18, 19, 20]. For example, Gómez-Bombarelli et al. [8] perform Bayesian optimization for maximizing the desired property, on the embedding space of molecule-generating variational auto-encoders. On the other hand, Guimaraes et al. [6] train a molecule-generating policy using reinforcement learning with the desired property formulated as a reward.

Intriguingly, several works [21, 22, 23] have recently evidenced that the traditional frameworks based on genetic algorithm (GA) can compete with or even outperform the recently proposed deep learning methods. They reveal that GA is effective, thanks to the powerful domain-specific genetic operators for exploring the chemical space. For example, Jensen [22] achieves outstanding performance by generating new molecules as a combination of subgraphs extracted from existing ones. Such observations also emphasize how domain knowledge can play a significant role in de novo molecular design. On the contrary, the current DNN-based methods do not exploit such domain knowledge explicitly; instead, they implicitly generalize the knowledge of high-rewarding molecules by training a DNN on them. Notably, the expressive power of DNN allows itself to parameterize a distribution over the whole molecular space flexibly.

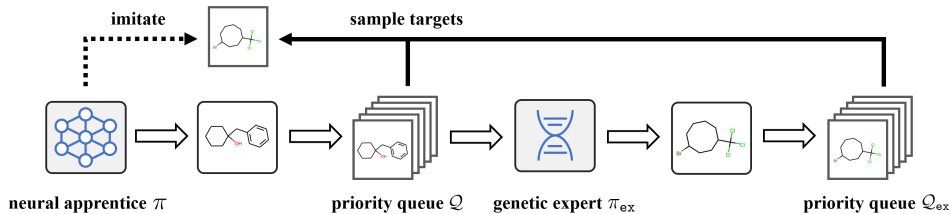


Figure 1: Illustration of the proposed genetic expert-guided learning (GEGL) framework.

Contribution. In this work, we propose genetic expert-guided learning (GEGL), which is a novel framework for training a molecule-generating DNN guided with genetic exploration. Our main idea is to formulate an *expert policy* by applying the domain-specific genetic operators, i.e., mutation and crossover,¹ to the DNN-generated molecules. Then the DNN becomes an *apprentice policy* that learns to imitate the highly-rewarding molecules discovered by the expert policy. Since the expert policy improves over the apprentice policy by design, the former policy consistently guides the latter policy to generate highly-rewarding molecules. We provide an overall illustration of our framework in Figure 1.

We note that our GEGL framework can be seen as a reinforcement learning algorithm with a novel mechanism for additional explorations. To be specific, the generation of a molecule can be regarded as an action and the desired property of the generated molecule as a reward. Similar to most reinforcement learning algorithms, reducing the sample complexity is crucial in our GEGL framework. To this end, we design our framework with *max-reward priority queues* [13, 24, 25, 26, 27]. By storing the highly-rewarding molecules, the priority queues prevent the policies from “forgetting” the valuable knowledge.

We extensively evaluate our method on four experiments: (a) optimization of penalized octanol-water partition coefficient, (b) optimization of penalized octanol-water partition coefficient under similarity constraints, (c) the GuacaMol benchmark [28] consisting of 20 de novo molecular design tasks, and (d) the GuacaMol benchmark evaluated under post-hoc filtering procedure [29]. Remarkably, our GEGL framework outperforms all prior methods for de novo molecular design by a large margin. In particular, GEGL achieves the penalized octanol-water partition coefficient score of 31.82, while the best baseline [16] and the second-best baseline [23] achieves the score of 26.1 and 20.72, respectively. For the GuacaMol benchmark, our algorithm achieves the highest score for 19 out of 20 tasks and newly achieves the perfect score for three tasks.

2 Related works

Automating the discovery of new molecules is likely to have significant impacts on essential applications such as drug discovery [1] and material design [2]. To achieve this, researchers have traditionally relied on *virtual screening* [30], which typically works in two steps: (a) enumerating all the possible combinations of predefined building-block molecules and (b) reporting the molecules with the desired property. However, the molecular space is large, and it is computationally prohibitive to enumerate and score the desired property for all the possible molecules.

De novo molecular design [4] methods attempt to circumvent this issue by generating a molecule from scratch. Instead of enumerating a large set of molecules, these methods search over the molecular space to maximize the desired property. In the following, we discuss the existing methods for de novo molecular design categorized by their optimization schemes: deep reinforcement learning, deep embedding optimization, and genetic algorithm.

Deep reinforcement learning (DRL). Deep reinforcement learning is arguably the most straightforward approach for solving the de novo molecular design problem with deep neural networks (DNNs) [6, 9, 13, 15, 17, 18]. Such methods formulate the generation of the molecules as a Markov decision process. In such formulations, the desired properties of molecules correspond to high rewards, and the policy learns to generate highly-rewarding molecules. We also note several works using deep reinforcement learning to solve combinatorial problems similar to the task of de novo molecular

¹See Figure 2 for illustrations of mutation and crossover.

design, e.g., program synthesis [25], combinatorial mathematics [31], biological sequence design [32], and protein structure design [33].

Deep embedding optimization (DEO). Also, there exist approaches to optimize molecular “embeddings” extracted from DNNs [7, 8, 10, 11, 12, 16, 19]. Such methods are based on training a neural network to learn a mapping between a continuous embedding space and a discrete molecular space. Then they apply optimization over the continuous embedding to maximize the desired property of the corresponding molecule. Methods such as gradient descent [10], Bayesian optimization [7, 8, 11, 12], constrained Bayesian optimization [19], and particle swarm optimization [16] have been applied for continuous optimization of the embedding space.

Genetic algorithm (GA). Inspired from the concept of natural selection, genetic algorithms (GAs) [21, 22, 34, 35, 36, 37, 38] search over the molecular space with genetic operators, i.e., mutation and crossover. To this end, the mutation randomly modifies an existing molecule, and the crossover randomly combines a pair of molecules. Such approaches are appealing since they are simple and capable of incorporating the domain knowledge provided by human experts. While the deep learning methods are gaining attention for de novo molecular design, several works [21, 22, 39] have recently demonstrated that GA can compete with or even outperform the DNN-based methods.

3 Genetic expert-guided learning (GEGL)

3.1 Overview of GEGL

In this section, we introduce genetic expert-guided learning (GEGL), a novel yet simple framework for de novo molecular design. To discover highly-rewarding molecules, GEGL aims at training a molecule-generating deep neural network (DNN). Especially, we design the framework using an additional genetic *expert policy*, which generates targets for imitation learning of the neural *apprentice policy*, i.e., the DNN. Our main idea is about formulating the expert policy as a “genetic improvement operator” applied to the apprentice policy; this allows us to steer the apprentice policy towards generating highly-rewarding molecules by imitating the better expert policy.

To apply our framework, we view de novo molecular design as a combinatorial optimization of discovering a molecule x , which maximizes the *reward* $r(x)$, i.e., the desired property.² To solve this problem, we collect highly-rewarding molecules from the neural apprentice policy $\pi(x; \theta)$ and the genetic expert policy $\pi_{\text{ex}}(x; \mathcal{X})$ throughout the learning process. Here, θ indicates the DNN’s parameter representing the apprentice policy, and \mathcal{X} indicates a set of “seed” molecules to apply the genetic operators for the expert policy. Finally, we introduce fixed-size *max-reward priority queues* \mathcal{Q} and \mathcal{Q}_{ex} , which are buffers that only keep a fixed number of molecules with the highest rewards.

Our GEGL framework repeats the following three-step procedure:

- Step A.** The apprentice policy $\pi(x; \theta)$ generates a set of molecules. Then the max-reward priority queue \mathcal{Q} with the size of K stores the generated molecules.
- Step B.** The expert policy $\pi_{\text{ex}}(x; \mathcal{Q})$ generates molecules using the updated priority queue \mathcal{Q} as the seed molecules. Next, the priority queue \mathcal{Q}_{ex} with a size of K stores the generated molecules.
- Step C.** The apprentice policy optimizes its parameter θ by learning to imitate the molecules sampled from the union of the priority queues $\mathcal{Q} \cup \mathcal{Q}_{\text{ex}}$. In other words, the parameter θ is updated to maximize $\sum_{x \in \mathcal{Q} \cup \mathcal{Q}_{\text{ex}}} \log \pi(x; \theta)$.

One may interpret GEGL as a deep reinforcement learning algorithm. From such a perspective, the corresponding Markov decision process has a fixed episode-length of one, and its action corresponds to the generation of a molecule. Furthermore, GEGL highly resembles the prior works on expert iteration [40, 41] and AlphaGo Zero [42], where the Monte Carlo tree search is used as an improvement operator that guides training through enhanced exploration. We provide an illustration and a detailed description of our algorithm in Figure 1 and Algorithm 1, respectively.

²In this paper, we consider the properties of molecules which can be measured quantitatively.

Algorithm 1 Genetic expert-guided learning (G EGL)

```
1: Set  $\mathcal{Q} \leftarrow \emptyset$ ,  $\mathcal{Q}_{\text{ex}} \leftarrow \emptyset$ . ▷ Initialize the max-reward priority queues  $\mathcal{Q}$  and  $\mathcal{Q}_{\text{ex}}$ .
2: for  $t = 1, \dots, T$  do
3:   for  $m = 1, \dots, M$  do ▷ Step A: add  $M$  samples generated by  $\pi$  into  $\mathcal{Q}$ .
4:     Update  $\mathcal{Q} \leftarrow \mathcal{Q} \cup \{\mathbf{x}\}$ , where  $\mathbf{x} \sim \pi(\mathbf{x}; \theta)$ .
5:     If  $|\mathcal{Q}| > K$ , update  $\mathcal{Q} \leftarrow \mathcal{Q} \setminus \{\mathbf{x}_{\min}\}$ , where  $\mathbf{x}_{\min} = \arg \min_{\mathbf{x} \in \mathcal{Q}} r(\mathbf{x})$ .
6:   end for
7:   for  $m = 1, \dots, M$  do ▷ Step B: add  $M$  samples generated by  $\pi_{\text{ex}}$  into  $\mathcal{Q}_{\text{ex}}$ .
8:     Update  $\mathcal{Q}_{\text{ex}} \leftarrow \mathcal{Q}_{\text{ex}} \cup \{\mathbf{x}\}$ , where  $\mathbf{x} \sim \pi_{\text{ex}}(\mathbf{x}; \mathcal{Q})$ .
9:     If  $|\mathcal{Q}_{\text{ex}}| > K$ , update  $\mathcal{Q}_{\text{ex}} \leftarrow \mathcal{Q}_{\text{ex}} \setminus \{\mathbf{x}_{\min}\}$ , where  $\mathbf{x}_{\min} = \arg \min_{\mathbf{x} \in \mathcal{Q}_{\text{ex}}} r(\mathbf{x})$ .
10:  end for
11:  Maximize  $\sum_{\mathbf{x} \in \mathcal{Q} \cup \mathcal{Q}_{\text{ex}}} \log \pi(\mathbf{x}; \theta)$  over  $\theta$ . ▷ Step C: train  $\pi$  with imitation learning.
12: end for
13: Report  $\mathcal{Q} \cup \mathcal{Q}_{\text{ex}}$  as the output. ▷ Output the highly-rewarding molecules.
```

3.2 Detailed components of G EGL

In the rest of this section, we provide a detailed description of each component in G EGL. We start by explaining our design choices on the expert and the apprentice policies. Then we discuss how the max-reward priority queues play an essential role in our framework.

Genetic expert policy. Our genetic expert policy $\pi_{\text{ex}}(x; \mathcal{X})$ is a distribution induced by applying the genetic operators, i.e., mutation and crossover, to a set of molecules \mathcal{X} . We use the genetic operators highly optimized (with domain knowledge) for searching over the molecular space; hence the expert policy efficiently improves over the apprentice policy in terms of exploration.

An adequate choice of genetic operators is crucial for the expert policy. While one can use any molecule-specific genetic operator, we choose the graph-based mutation and crossover proposed by Jensen [22], as they recently demonstrated outstanding performance for de novo molecular design. At a high-level, the genetic expert policy $\pi_{\text{ex}}(x; \mathcal{X})$ generates a molecule in two steps. First, the expert policy generates a *child* molecule by applying the crossover to a pair of *parent* molecules randomly drawn from \mathcal{X} . To be specific, two subgraphs extracted from the parents attach to form a child molecule. Next, with a small probability, the expert policy mutates the child by atom-wise or bond-wise modification, e.g., adding an atom. We provide an illustration and a detailed description of the genetic operators in Figure 2 and Appendix A, respectively.

Neural apprentice policy. We parameterize our neural apprentice policy using a long-short term memory (LSTM) network [43]. Moreover, the molecules are represented by a sequence of characters, i.e., the simplified molecular-input line-entry system (SMILES) [44] format. Under such a design, the probability $\pi(\mathbf{x}; \theta)$ of a molecule \mathbf{x} being generated from the apprentice policy is factorized into $\prod_{n=1}^N \pi(x_n | x_1, \dots, x_{n-1}; \theta)$. Here, x_1, \dots, x_N are the characters corresponding to canonical SMILES representation of the given molecule.

We note that our choice of using the LSTM network to generate SMILES representations of molecules might not seem evident. Especially, molecular graph representations alternatively express the molecule, and many works have proposed new molecule-generating graph neural networks (GNNs) [8, 12, 15, 18, 45, 46]. However, no particular GNN architecture clearly dominates over others, and recent molecular generation benchmarks [28, 47] report that the LSTM network matches (or improves over) the performance of GNNs. Therefore, while searching for the best molecule-generating DNN architecture is a significant research direction, we leave it for future work. Instead, we choose the well-established LSTM architecture for the apprentice policy.

Max-reward priority queues. Role of the max-reward priority queues \mathcal{Q} and \mathcal{Q}_{ex} in our framework is twofold. First, the priority queues provide highly-rewarding molecules for the expert and the apprentice policy. Furthermore, they prevent the policies from “forgetting” the highly-rewarding molecules observed in prior. Recent works [13, 24, 25, 26, 27] have also shown similar concepts to be successful for learning in deterministic environments.

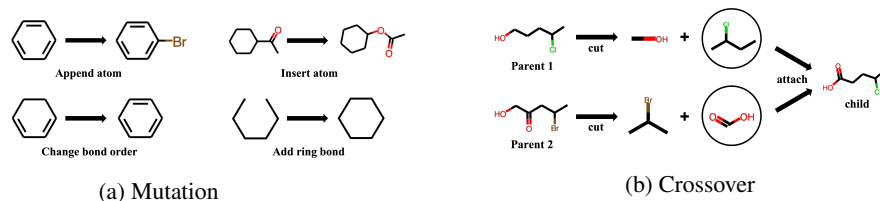


Figure 2: Illustration of (a) mutation and (b) crossover used in the genetic expert policy.

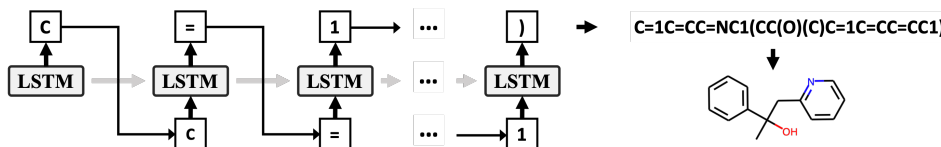


Figure 3: Illustration of the apprentice policy generating a SMILES representation of a molecule.

We further elaborate on our choice of training the apprentice policy on the union of the priority queues $\mathcal{Q} \cup \mathcal{Q}_{\text{ex}}$ instead of the priority queue \mathcal{Q}_{ex} . This choice comes from how the expert policy does not always improve the apprentice policy in terms of reward, although it does in terms of exploration. Hence, it is beneficial for the apprentice policy to imitate the highly-rewarding molecules generated from both the apprentice and the expert policy. This promotes the apprentice to be trained on molecules with improved rewards.

4 Experiments

In this section, we report the experimental results of the proposed genetic expert-guided learning (GEG) framework. To this end, we extensively compare GEG with the existing works, for the optimization of the penalized octanol-water partition coefficient [48] and the GuacaMol benchmark [28]. We also provide additional experimental results in Appendix B; these results consist of relatively straightforward tasks such as targeted optimization of the octanol-water partition coefficient and optimization of the quantitative estimate of drug-likeness (QED) [49]. For comparison, we consider a variety of existing works on de novo molecular design based on deep reinforcement learning (DRL), deep embedding optimization (DEO), genetic algorithm (GA), and deep supervised learning (DSL).³ We report the numbers obtained by the existing works unless stated otherwise. We also provide descriptions of the GEG implementation and the employed baselines in Appendix C and D, respectively.

4.1 Optimization of penalized octanol-water partition coefficient

Comparing to the literature standard, we aim at maximizing the *penalized octanol-water partition coefficient* (PenalizedLogP) score defined as follows:

$$\text{PenalizedLogP}(x) = \text{LogP}(x) - \text{SyntheticAccessibility}(x) - \text{RingPenalty}(x),$$

where LogP , $\text{SyntheticAccessibility}$, and RingPenalty correspond to the (unpenalized) octanol-water partition coefficient [52], the synthetic accessibility [53] penalty, and the penalty for atom rings of size larger than 6. We also note that Gómez-Bombarelli et al. [48] first performed this task motivated by how the octanol-water partition coefficient plays an important role in characterizing the drug-likeness of a molecule.

Unconstrained optimization. First, we attempt to find a molecule maximizing the PenalizedLogP score as the objective without specific constraints. We limit our framework to generate molecules with at most 81 SMILES characters (as done by Jensen [22], Nigam et al. [23], and Yang et al. [50]). In Table 1a, we observe that our algorithm indeed outperforms the existing baselines by a large margin. In particular, GEG achieves a score of 31.82, which relatively outperforms the second-best (MSO) and the third-best (DA-GA) baselines by 22% and 53%, respectively. This result highlights the strong performance of GEG.

³DSL-based methods train DNNs to imitate highly-rewarding molecules provided as supervisions.

Table 1: Experimental results on the optimization of (a) PenalizedLogP and (b) PenalizedLogP with similarity constraint of δ . Types of the algorithms are indicated by deep reinforcement learning (DRL), deep embedding optimization (DEO), deep supervised learning (DSL), and genetic algorithm (GA). ^{†‡}We report the average and standard deviation of the objectives collected over five independent runs and 800 molecules for (a) and (b), respectively. *For GraphAF, we re-evaluate the official implementation (See Appendix E).

(a) PenalizedLogP			(b) Similarity-constrained PenalizedLogP				
Algorithm	Type	Objective	δ	Algorithm	Type	Objective	Succ. rate
GVAE+BO [Kusner et al. 2017]	DEO	2.87 \pm 0.06	0.4	JT-VAE [Jin et al. 2018]	DEO	0.84 \pm 1.45	0.84
SD-VAE [Dai et al. 2018]	DEO	3.50 \pm 0.44		GraphAF* [Shi et al. 2020]	DRL	1.98 \pm 1.34	1.00
ORGAN [Guimaraes et al. 2017]	DRL	3.52 \pm 0.08		GCPN [You et al. 2018]	DRL	2.49 \pm 1.30	1.00
VAE+CBO [Griffiths and Hernández-Lobato 2020]	DEO	4.01		MolDQN [Zhou et al. 2019]	DRL	3.37 \pm 1.62	1.00
ChemGE [Yoshikawa et al. 2018]	GA	4.53 \pm 0.26		DEFactor [Assouel et al. 2018]	DEO	3.41 \pm 1.67	0.86
CVAE+BO [Gómez-Bombarelli et al. 2018]	DEO	4.85 \pm 0.17		VJTNN [Jin et al. 2019]	DSL	3.55 \pm 1.67	-
JT-VAE [Jin et al. 2018]	DEO	4.90 \pm 0.33		HierG2G [Jin et al. 2020]	DSL	3.98 \pm 1.09	-
ChemTS [Yang et al. 2017]	DRL	5.6 \pm 0.5		DA-GA [Nigam et al. 2020]	GA	5.93 \pm 1.41	1.00
GCPN [You et al. 2018]	DRL	7.86 \pm 0.07		GEGL [‡] (Ours)	DRL	7.37 \pm 1.22	1.00
MRNN [Popova et al. 2019]	DRL	8.63		0.6	JT-VAE [Jin et al. 2018]	DEO	0.21 \pm 0.71
MolDQN [Zhou et al. 2019]	DRL	11.84	GCPN [You et al. 2018]		DRL	0.79 \pm 0.63	1.00
GraphAF [Shi et al. 2020]	DRL	12.23	DEFactor [Assouel et al. 2018]		DEO	1.55 \pm 1.19	0.73
GB-GA [Jensen 2019]	GA	15.76 \pm 5.76	GraphAF* [Shi et al. 2020]		DRL	1.68 \pm 1.22	0.97
DA-GA [Nigam et al. 2020]	GA	20.72 \pm 3.14	MolDQN [Zhou et al. 2019]		DRL	1.85 \pm 1.21	1.00
MSO [Winter et al. 2019]	DEO	26.1	VJTNN [Jin et al. 2019]		DSL	2.33 \pm 1.17	-
GEGL [†] (Ours)	DRL	31.82 \pm 0.01	HierG2G [Jin et al. 2020]		DSL	2.49 \pm 1.46	-
			DA-GA [Nigam et al. 2020]		GA	3.44 \pm 1.09	1.00
			GEGL [‡] (Ours)		DRL	3.98 \pm 1.22	1.00

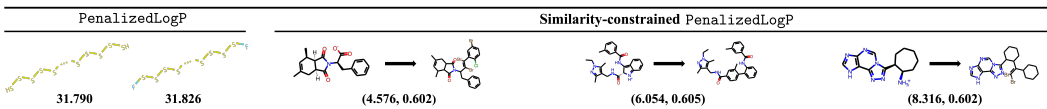


Figure 4: Illustration of the highly-scoring molecule and (reference molecule, improved molecule) for the unconstrained and similarity-constrained PenalizedLogP optimization, respectively. Below each molecule, we denote the associated objective and (objective, similarity) for the unconstrained and similarity-constrained PenalizedLogP optimization, respectively.

Constrained optimization. In this experiment, we follow the experimental setup proposed by Jin et al. [12]. Namely, for each molecule x_{ref} from 800 low-PenalizedLogP-scoring molecules from the ZINC data set [54], we search for a new molecule x with the maximum PenalizedLogP score while being constrained to be similar to the reference molecule x_{ref} . To be specific, we express this optimization as follows:

$$\max_x \text{PenalizedLogP}(x) - \text{PenalizedLogP}(x_{\text{ref}}), \quad \text{s.t.} \quad \text{Similarity}(x, x_{\text{ref}}) \geq \delta,$$

where $\text{Similarity}(\cdot, \cdot)$ is the Tanimoto similarity score [55]. We report the above objective averaged over the 800 molecules. We also evaluate the “success ratio” of the algorithms, i.e., the ratio of molecules with a positive objective.

In Table 1b, we once again observe GEGL to achieve superior performance to the existing algorithms. We also note that our algorithm always succeeds in improving the PenalizedLogP score of the reference molecule, i.e., the success ratio is 1.00.

Generated molecules. We now report the molecules generated for unconstrained and constrained optimization of PenalizedLogP score in Figure 4. Notably, for unconstrained optimization, we observe that our model produces “unrealistic” molecules that contain a long chain of sulfurs. This symptom arise from our method exploiting the ambiguity of the PenalizedLogP score, i.e., the score spuriously assigning high values to the unrealistic molecules. Indeed, similar observations (on algorithms generating a long chain of sulfurs) have been made regardless of optimization methods for de novo molecular design. For example, Shi et al. [18], Winter et al. [16], and Nigam et al. [23] reported molecules with similar structure when using deep reinforcement learning, deep embedding optimization, and genetic algorithm, respectively. Such an observation emphasizes why one should carefully design the procedure of de novo molecular design.

Table 2: Experimental results for task-ids of 1, 2, . . . , 20 from (a) the GuacaMol benchmark and (b) the GuacaMol benchmark evaluated with post-hoc filtering process. See Appendix F for the description of each task per id. *We re-evaluate the official implementation for baselines in (b).

(a) GuacaMol									(b) GuacaMol with filtering				
id	ChEMBL [56]	MCTS [22]	ChemGE [21]	HC-MLE [13]	GB-GA [22]	MSO [16]	CREM [39]	GEGL (Ours)	ChEMBL* [56]	ChemGE* [21]	HC-MLE* [13]	GB-GA* [22]	GEGL (Ours)
1	0.505	0.355	0.732	1.000	1.000	1.000	1.000	1.000	0.505	0.646	1.000	1.000	1.000
2	0.418	0.311	0.515	1.000	1.000	1.000	1.000	1.000	0.260	0.504	0.537	0.837	0.552
3	0.456	0.311	0.598	1.000	1.000	1.000	1.000	1.000	0.456	0.552	1.000	1.000	1.000
4	0.595	0.380	0.834	1.000	1.000	1.000	1.000	1.000	0.595	0.769	1.000	0.995	1.000
5	0.719	0.749	0.907	1.000	1.000	1.000	1.000	1.000	0.711	0.959	1.000	0.996	1.000
6	0.629	0.402	0.790	1.000	1.000	1.000	1.000	1.000	0.632	0.631	1.000	0.996	1.000
7	0.684	0.410	0.829	0.993	0.971	0.997	0.966	1.000	0.684	0.786	0.997	0.960	1.000
8	0.747	0.632	0.889	0.879	0.982	1.000	0.940	1.000	0.747	0.883	0.992	0.823	1.000
9	0.334	0.225	0.334	0.438	0.406	0.437	0.371	0.455	0.334	0.361	0.453	0.402	0.455
10	0.351	0.170	0.380	0.422	0.432	0.395	0.434	0.437	0.351	0.377	0.433	0.420	0.437
11	0.839	0.784	0.886	0.907	0.953	0.966	0.995	1.000	0.839	0.895	0.916	0.914	1.000
12	0.817	0.695	0.931	0.959	0.998	1.000	1.000	1.000	0.815	0.920	0.999	0.905	1.000
13	0.792	0.616	0.881	0.855	0.920	0.931	0.969	0.958	0.786	0.714	0.882	0.530	0.933
14	0.575	0.385	0.661	0.808	0.792	0.834	0.815	0.882	0.572	0.572	0.835	0.780	0.833
15	0.696	0.533	0.722	0.894	0.894	0.900	0.902	0.924	0.679	0.709	0.902	0.889	0.905
16	0.509	0.458	0.689	0.545	0.891	0.868	0.763	0.922	0.501	0.587	0.601	0.634	0.749
17	0.547	0.488	0.413	0.669	0.754	0.764	0.770	0.834	0.547	0.647	0.715	0.698	0.763
18	0.259	0.040	0.552	0.978	0.990	0.994	0.994	1.000	0.127	0.827	0.992	0.789	1.000
19	0.933	0.590	0.970	0.996	1.000	1.000	1.000	1.000	0.933	0.857	1.000	0.994	1.000
20	0.738	0.470	0.885	0.998	1.000	1.000	1.000	1.000	0.690	0.964	1.000	1.000	1.000

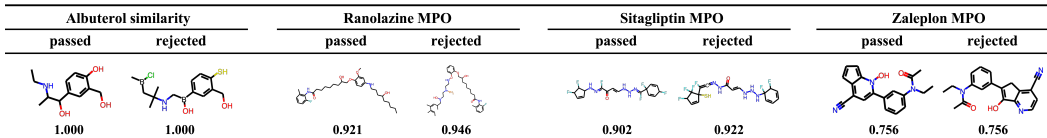


Figure 5: Illustration of the molecules generated for the GuacaMol benchmark, that have passed and rejected from the filtering procedure. Below each molecule, we also denote the associated objectives.

4.2 GuacaMol benchmark

Next, we provide the empirical results for the GuacaMol benchmark [28], designed specifically to measure the performance of de novo molecular design algorithms. It consists of 20 chemically meaningful molecular design tasks, that have been carefully designed and studied by domain-experts in the past literature [38, 45, 57, 58, 59]. Notably, the GuacaMol benchmark scores a set of molecules rather than a single one, to evaluate the algorithms’ ability to produce diverse molecules. We further provide details on the benchmark in Appendix F.

Benchmark results. In Table 2, we observe that GEGL outperforms the existing baselines by a large margin. Namely, GEGL achieves the highest score for 19 out of 20 tasks. Furthermore, our algorithm perfectly solves thirteen tasks,⁴ where three of them were not known to be perfectly solved. Such a result demonstrates how our algorithm effectively produces a high-rewarding and diverse set of molecules.

Evaluation with post-hoc filtering. As observed in Section 4.1 and prior works, de novo molecular design algorithms may lead to problematic results. For example, the generated molecules may be chemically reactive, hard to synthesize, or perceived to be “unrealistic” to domain experts. To consider this aspect, we evaluate our algorithm under the post-hoc filtering approach [29]. Specifically, we use the expert-designed filter to reject the molecules with undesirable feature. In other words, we train the models as in Table 2, but only report the performance of generated molecules that pass the filter. Since the filtering procedure is post-hoc, the de novo molecular design algorithms will not be able to aggressively exploit possible ambiguities of the filtering process. We further describe the filtering procedure in Appendix F.

As shown in Table 2b, GEGL still outperforms the baselines even when the undesirable molecules are filtered out. This validates the ability of our algorithm to generate chemically meaningful results. Hence, we conclude that our GEGL can be used flexibly with various choice of de novo molecular design process.

⁴Every score is normalized to be in the range of [0, 1].

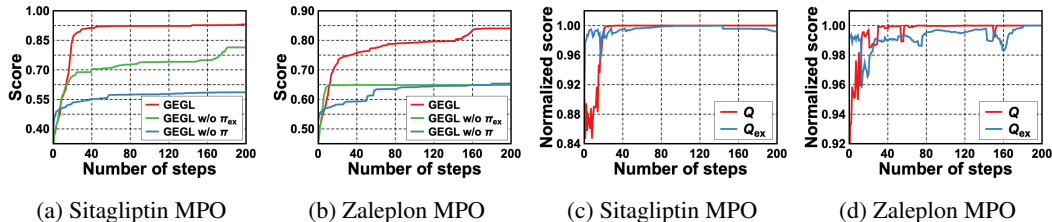


Figure 6: Illustration of ablation studies for (a, b) investigating contribution from DNN and genetic operator, and (c, d) separate evaluation of max-reward priority queues.

Generated molecules. In Figure 5, we illustrate the high-scoring molecules generated by GEGL for the Albuterol similarity, Ranolazine MPO, Sitagliptin MPO, and Zaleplon MPO tasks from the GuacaMol benchmark (corresponding to task-ids of 4, 13, 15, 16 in Table 2). Note that the filters used in Table 2b provide reasons for rejection of the molecules. For example, the high-scoring molecule from the Zaleplon MPO task was rejected due to containing a SMILES of C=C, i.e., *enol*. This is undesirable, as many enols have been shown to be reactive [60]. See Appendix G for further explanation of the molecules being passed and rejected from the post-hoc filtering process.

4.3 Ablation studies

Finally, we perform ablation studies on our algorithm to investigate the behavior of each component. To this end, we conduct experiments on the Sitagliptin MPO and Zaleplon MPO tasks from the GuacaMol benchmark. Note that Sitagliptin MPO and Zaleplon MPO tasks corresponds to task-ids of 15 and 16 in Table 2, respectively.

Contribution from the DNN and the genetic operator. We start by inspecting the contribution of the DNN and the genetic operator in our algorithm. To this end, we compare GEGL with (a) GEGL without the expert policy π_{ex} and (b) GEGL without the apprentice policy π . To be specific, (a) trains the apprentice policy to imitate the highly-rewarding molecules generated by itself. On the other hand, (b) freezes the max-reward priority queue Q by the highly-rewarding samples from the ChEMBLE dataset [56], then only updates Q_{ex} based on the expert policy.⁵ In Figure 6a and 6b, we observe that (a) and (b) performs significantly worse than GEGL. This result confirms that the neural apprentice policy and the genetic expert policy bring mutual benefits to our framework.

Separate evaluation of the max-reward priority queues. Next, we describe behavior of the apprentice policy and the expert policy during training. To this end, we compare the GuacaMol scores for the priority queues Q and Q_{ex} that are normalized by the original GEGL score. For example, we consider $\frac{\text{GuacaMolScore}(Q)}{\text{GuacaMolScore}(Q \cup Q_{\text{ex}})}$ for evaluating Q where $\text{GuacaMolScore}(\cdot)$ is the GuacaMol score evaluated on a set of molecules.

In Figure 6c and 6d, we observe that the samples collected from the genetic expert policy, i.e., Q_{ex} , indeed improves over that of the apprentice policy, i.e., Q during early stages of the training. However, as the training goes on, the apprentice policy learns to generate molecules with quality higher than that of the expert policy. Since Table 6a and 6b shows that apprentice policy cannot reach the same performance without the expert policy, one may conclude that the apprentice policy effectively learns to comprise the benefits of genetic operators through learning.

5 Conclusion

We propose a new framework based on deep neural networks (DNNs) to solve the de novo molecular design problem. Our main idea is to enhance the training of DNN with domain knowledge, using the powerful expert-designed genetic operators to guide the training of the DNN. Through extensive experiments, our algorithm demonstrates state-of-the-art performance across a variety of tasks. We believe extending our framework to combinatorial search problems where strong genetic operators exist, e.g., biological sequence design [61], program synthesis [62], and vehicle routing problems [63], would be both promising and interesting.

⁵Note that one can further modify (b) to obtain a proper genetic algorithm proposed by Jensen [22], but we omit this comparison since it was done in Table 2.

Broader Impact

De novo molecular design. Our framework is likely to advance the field of de novo molecular design. In this field, successful algorithms significantly impact real-world, since the discovery of a new molecule has been the key challenge of many applications. Domain of such applications includes, but are not limited to, drug molecules [64], organic light emitting diodes [65], organic solar cells [66], energetic materials [67], and electrochromic devices [68]. Improvements in these applications are beneficial to human kind in general, as they often improve the quality of human life and may broaden our knowledge of chemistry.

However, one should always take care in automating such molecular design processes despite its promise, especially when using a deep neural network (DNN) to synthesize molecules in a fully automated way. Currently, there is no ways of entirely explaining and regularizing the behavior of DNNs in general. Hence, DNN-based de novo molecular design might cause safety issues from unexpected behaviors and these aspect should be taken into consideration. While such an issue is resolvable by human experts inspecting the proposals of the DNN, we would also like to encourage the researchers to develop a “safe” framework for de novo molecular design.

Combinatorial optimization with deep reinforcement learning. In a broader sense, our framework offers a new paradigm to search over a intractably large space of combinatorial objects with DNN. In particular, our algorithm is expected to perform well for domains where genetic algorithms are powerful; this includes domains of biological sequence design [61], program synthesis [62], and vehicle routing problems [63]. Hence, at a high-level, our work also shares the domain of applications impacted from such works.

More specifically, we follow the frameworks that use DNN to solve such combinatorial optimization problems. While these methods are certainly promising, we note the potential pitfall of overlooking the traditional solvers, due to the recent enthusiasm focused around deep neural networks. Furthermore, as observed in by several recent works [22, 69], the domain-specific methods may outperform the DNN-based methods, due to containing an important knowledge about the target problem as a strong prior. Hence, we would like to recommend the researchers to carefully apply their DNN-based methods for solving such problems, considering the domain-specific knowledge in mind.

References

- [1] James P Hughes, Stephen Rees, S Barrett Kalindjian, and Karen L Philpott. Principles of early drug discovery. *British journal of pharmacology*, 162(6):1239–1249, 2011.
- [2] Cenqi Yan, Stephen Barlow, Zhaohui Wang, He Yan, Alex K-Y Jen, Seth R Marder, and Xiaowei Zhan. Non-fullerene acceptors for organic solar cells. *Nature Reviews Materials*, 3(3):1–19, 2018.
- [3] Regine S Bohacek, Colin McMartin, and Wayne C Guida. The art and practice of structure-based drug design: a molecular modeling perspective. *Medicinal research reviews*, 16(1):3–50, 1996.
- [4] Gisbert Schneider and Uli Fechner. Computer-based de novo design of drug-like molecules. *Nature Reviews Drug Discovery*, 4(8):649–663, 2005.
- [5] Gisbert Schneider. *De novo molecular design*. John Wiley & Sons, 2013.
- [6] Gabriel Lima Guimaraes, Benjamin Sanchez-Lengeling, Carlos Outeiral, Pedro Luis Cunha Farias, and Alán Aspuru-Guzik. Objective-reinforced generative adversarial networks (organ) for sequence generation models. *arXiv preprint arXiv:1705.10843*, 2017.
- [7] Matt J Kusner, Brooks Paige, and José Miguel Hernández-Lobato. Grammar variational autoencoder. In *International Conference on Machine Learning*, pages 1945–1954, 2017.
- [8] Rafael Gómez-Bombarelli, Jennifer N Wei, David Duvenaud, José Miguel Hernández-Lobato, Benjamín Sánchez-Lengeling, Dennis Sheberla, Jorge Aguilera-Iparraguirre, Timothy D Hirzel, Ryan P Adams, and Alán Aspuru-Guzik. Automatic chemical design using a data-driven continuous representation of molecules. *ACS central science*, 4(2):268–276, 2018.

- [9] Jiaxuan You, Bowen Liu, Zhitao Ying, Vijay Pande, and Jure Leskovec. Graph convolutional policy network for goal-directed molecular graph generation. In *Advances in Neural Information Processing Systems*, pages 6410–6421, 2018.
- [10] Qi Liu, Miltiadis Allamanis, Marc Brockschmidt, and Alexander Gaunt. Constrained graph variational autoencoders for molecule design. In *Advances in Neural Information Processing Systems*, pages 7795–7804, 2018.
- [11] Hanjun Dai, Yingtao Tian, Bo Dai, Steven Skiena, and Le Song. Syntax-directed variational autoencoder for structured data. In *International Conference on Learning Representations*, 2018. URL <https://openreview.net/forum?id=SyqShMZRBb>.
- [12] Wengong Jin, Regina Barzilay, and Tommi Jaakkola. Junction tree variational autoencoder for molecular graph generation. In *International Conference on Machine Learning*, pages 2323–2332, 2018.
- [13] Daniel Neil, Marwin Segler, Laura Guasch, Mohamed Ahmed, Dean Plumbley, Matthew Sellwood, and Nathan Brown. Exploring deep recurrent models with reinforcement learning for molecule design, 2018. URL <https://openreview.net/forum?id=HkcTe-bR->.
- [14] Rim Assouel, Mohamed Ahmed, Marwin H Segler, Amir Saffari, and Yoshua Bengio. De-factor: Differentiable edge factorization-based probabilistic graph generation. *arXiv preprint arXiv:1811.09766*, 2018.
- [15] Mariya Popova, Mykhailo Shvets, Junier Oliva, and Olexandr Isayev. Molecularrrn: Generating realistic molecular graphs with optimized properties. *arXiv preprint arXiv:1905.13372*, 2019.
- [16] Robin Winter, Floriane Montanari, Andreas Steffen, Hans Briem, Frank Noé, and Djork-Arné Clevert. Efficient multi-objective molecular optimization in a continuous latent space. *Chemical science*, 10(34):8016–8024, 2019.
- [17] Zhenpeng Zhou, Steven Kearnes, Li Li, Richard N Zare, and Patrick Riley. Optimization of molecules via deep reinforcement learning. *Scientific reports*, 9(1):1–10, 2019.
- [18] Chence Shi, Minkai Xu, Zhaocheng Zhu, Weinan Zhang, Ming Zhang, and Jian Tang. Graphaf: a flow-based autoregressive model for molecular graph generation. In *International Conference on Learning Representations*, 2020. URL <https://openreview.net/forum?id=S1esMkHYPr>.
- [19] Ryan-Rhys Griffiths and José Miguel Hernández-Lobato. Constrained bayesian optimization for automatic chemical design using variational autoencoders. *Chemical Science*, 2020.
- [20] Wengong Jin, Regina Barzilay, and Tommi Jaakkola. Hierarchical generation of molecular graphs using structural motifs. In *International Conference on Machine Learning*, page to appear, 2020.
- [21] Naruki Yoshikawa, Kei Terayama, Masato Sumita, Teruki Homma, Kenta Oono, and Koji Tsuda. Population-based de novo molecule generation, using grammatical evolution. *Chemistry Letters*, 47(11):1431–1434, 2018.
- [22] Jan H Jensen. A graph-based genetic algorithm and generative model/monte carlo tree search for the exploration of chemical space. *Chemical science*, 10(12):3567–3572, 2019.
- [23] AkshatKumar Nigam, Pascal Friederich, Mario Krenn, and Alan Aspuru-Guzik. Augmenting genetic algorithms with deep neural networks for exploring the chemical space. In *International Conference on Learning Representations*, 2020. URL <https://openreview.net/forum?id=H1lmyRNFvr>.
- [24] Anvita Gupta and James Zou. Feedback gan for dna optimizes protein functions. *Nature Machine Intelligence*, 1(2):105–111, 2019.
- [25] Chen Liang, Jonathan Berant, Quoc Le, Kenneth Forbus, and Ni Lao. Neural symbolic machines: Learning semantic parsers on freebase with weak supervision. In *Proceedings of the 55th Annual Meeting of the Association for Computational Linguistics (Volume 1: Long Papers)*, pages 23–33, 2017.

- [26] Daniel A Abolafia, Mohammad Norouzi, Jonathan Shen, Rui Zhao, and Quoc V Le. Neural program synthesis with priority queue training. *arXiv preprint arXiv:1801.03526*, 2018.
- [27] Rishabh Agarwal, Chen Liang, Dale Schuurmans, and Mohammad Norouzi. Learning to generalize from sparse and underspecified rewards. In *International Conference on Machine Learning*, pages 130–140, 2019.
- [28] Nathan Brown, Marco Fiscato, Marwin HS Segler, and Alain C Vaucher. Guacamol: benchmarking models for de novo molecular design. *Journal of chemical information and modeling*, 59(3):1096–1108, 2019.
- [29] Wenhao Gao and Connor W Coley. The synthesizability of molecules proposed by generative models. *Journal of Chemical Information and Modeling*, 2020.
- [30] Brian K Shoichet. Virtual screening of chemical libraries. *Nature*, 432(7019):862–865, 2004.
- [31] Irwan Bello, Hieu Pham, Quoc V Le, Mohammad Norouzi, and Samy Bengio. Neural combinatorial optimization with reinforcement learning. *arXiv preprint arXiv:1611.09940*, 2016.
- [32] Christof Angermueller, David Dohan, David Belanger, Ramya Deshpande, Kevin Murphy, and Lucy Colwell. Model-based reinforcement learning for biological sequence design. In *International Conference on Learning Representations*, 2020. URL <https://openreview.net/forum?id=HklxbgBKvr>.
- [33] David Brookes, Hahnbeom Park, and Jennifer Listgarten. Conditioning by adaptive sampling for robust design. In *International Conference on Machine Learning*, pages 773–782, 2019.
- [34] David Weininger. Method and apparatus for designing molecules with desired properties by evolving successive populations, July 18 1995. US Patent 5,434,796.
- [35] Al Globus, John Lawton, and Todd Wipke. Automatic molecular design using evolutionary techniques. *Nanotechnology*, 10(3):290, 1999.
- [36] Dominique Douguet, Etienne Thoreau, and Gérard Grassy. A genetic algorithm for the automated generation of small organic molecules: Drug design using an evolutionary algorithm. *Journal of computer-aided molecular design*, 14(5):449–466, 2000.
- [37] Gisbert Schneider, Man-Ling Lee, Martin Stahl, and Petra Schneider. De novo design of molecular architectures by evolutionary assembly of drug-derived building blocks. *Journal of computer-aided molecular design*, 14(5):487–494, 2000.
- [38] Nathan Brown, Ben McKay, François Gilardoni, and Johann Gasteiger. A graph-based genetic algorithm and its application to the multiobjective evolution of median molecules. *Journal of chemical information and computer sciences*, 44(3):1079–1087, 2004.
- [39] Pavel Polishchuk. Crem: chemically reasonable mutations framework for structure generation. *Journal of Cheminformatics*, 12:1–18, 2020.
- [40] Thomas Anthony, Zheng Tian, and David Barber. Thinking fast and slow with deep learning and tree search. In *Advances in Neural Information Processing Systems*, pages 5360–5370, 2017.
- [41] Thomas Anthony, Robert Nishihara, Philipp Moritz, Tim Salimans, and John Schulman. Policy gradient search: Online planning and expert iteration without search trees. *arXiv preprint arXiv:1904.03646*, 2019.
- [42] David Silver, Julian Schrittwieser, Karen Simonyan, Ioannis Antonoglou, Aja Huang, Arthur Guez, Thomas Hubert, Lucas Baker, Matthew Lai, Adrian Bolton, et al. Mastering the game of go without human knowledge. *Nature*, 550(7676):354–359, 2017.
- [43] Sepp Hochreiter and Jürgen Schmidhuber. Long short-term memory. *Neural computation*, 9(8):1735–1780, 1997.
- [44] David Weininger. Smiles, a chemical language and information system. 1. introduction to methodology and encoding rules. *Journal of chemical information and computer sciences*, 28(1):31–36, 1988.

- [45] Marwin HS Segler, Thierry Kogej, Christian Tyrchan, and Mark P Waller. Generating focused molecule libraries for drug discovery with recurrent neural networks. *ACS central science*, 4(1): 120–131, 2018.
- [46] Kaushalya Madhawa, Katushiko Ishiguro, Kosuke Nakago, and Motoki Abe. Graphnvp: An invertible flow model for generating molecular graphs. *arXiv preprint arXiv:1905.11600*, 2019.
- [47] Daniil Polykovskiy, Alexander Zhebrak, Benjamin Sanchez-Lengeling, Sergey Golovanov, Oktai Tatanov, Stanislav Belyaev, Rauf Kurbanov, Aleksey Artamonov, Vladimir Aladinskiy, Mark Veselov, et al. Molecular sets (moses): a benchmarking platform for molecular generation models. *arXiv preprint arXiv:1811.12823*, 2018.
- [48] Rafael Gómez-Bombarelli, Jennifer N. Wei, David Duvenaud, José Miguel Hernández-Lobato, Benjamín Sánchez-Lengeling, Dennis Sheberla, Jorge Aguilera-Iparraguirre, Timothy D. Hirzel, Ryan P. Adams, and Alán Aspuru-Guzik. Automatic chemical design using a data-driven continuous representation of molecules, 2016.
- [49] G Richard Bickerton, Gaia V Paolini, Jérémy Besnard, Sorel Muresan, and Andrew L Hopkins. Quantifying the chemical beauty of drugs. *Nature chemistry*, 4(2):90, 2012.
- [50] Xiufeng Yang, Jinzhe Zhang, Kazuki Yoshizoe, Kei Terayama, and Koji Tsuda. Chemts: an efficient python library for de novo molecular generation. *Science and technology of advanced materials*, 18(1):972–976, 2017.
- [51] Wengong Jin, Kevin Yang, Regina Barzilay, and Tommi Jaakkola. Learning multimodal graph-to-graph translation for molecule optimization. In *International Conference on Learning Representations*, 2019. URL <https://openreview.net/forum?id=B1xJAsA5F7>.
- [52] Younggil Kwon. *Handbook of essential pharmacokinetics, pharmacodynamics and drug metabolism for industrial scientists*. Springer Science & Business Media, 2001.
- [53] Peter Ertl and Ansgar Schuffenhauer. Estimation of synthetic accessibility score of drug-like molecules based on molecular complexity and fragment contributions. *Journal of cheminformatics*, 1(1):8, 2009.
- [54] John J Irwin, Teague Sterling, Michael M Mysinger, Erin S Bolstad, and Ryan G Coleman. Zinc: a free tool to discover chemistry for biology. *Journal of chemical information and modeling*, 52(7):1757–1768, 2012.
- [55] Taffee T Tanimoto. Elementary mathematical theory of classification and prediction. 1958.
- [56] Anna Gaulton, Louisa J Bellis, A Patricia Bento, Jon Chambers, Mark Davies, Anne Hersey, Yvonne Light, Shaun McGlinchey, David Michalovich, Bissan Al-Lazikani, et al. ChEMBL: a large-scale bioactivity database for drug discovery. *Nucleic acids research*, 40(D1):D1100–D1107, 2012.
- [57] Andrea Zaliani, Krisztina Boda, Thomas Seidel, Achim Herwig, Christof H Schwab, Johann Gasteiger, Holger Claußen, Christian Lemmen, Jörg Degen, Juri Pärn, et al. Second-generation de novo design: a view from a medicinal chemist perspective. *Journal of computer-aided molecular design*, 23(8):593–602, 2009.
- [58] Peter Willett, John M Barnard, and Geoffrey M Downs. Chemical similarity searching. *Journal of chemical information and computer sciences*, 38(6):983–996, 1998.
- [59] Johann Gasteiger and Thomas Engel. *Cheminformatics: a textbook*. John Wiley & Sons, 2006.
- [60] Isao Kuwajima and Eiichi Nakamura. Reactive enolates from enol silyl ethers. *Accounts of Chemical Research*, 18(6):181–187, 1985.
- [61] Rune B Lyngsø, James WJ Anderson, Elena Sizikova, Amarendra Badugu, Tomas Hyland, and Jotun Hein. Frnakenstein: multiple target inverse rna folding. *BMC bioinformatics*, 13(1):260, 2012.

- [62] Thomas Helmuth and Lee Spector. General program synthesis benchmark suite. In *Proceedings of the 2015 Annual Conference on Genetic and Evolutionary Computation*, pages 1039–1046, 2015.
- [63] Christian Prins. A simple and effective evolutionary algorithm for the vehicle routing problem. *Computers & Operations Research*, 31(12):1985–2002, 2004.
- [64] Edward J Griffen, Alexander G Dossetter, Andrew G Leach, and Shane Montague. Can we accelerate medicinal chemistry by augmenting the chemist with big data and artificial intelligence? *Drug discovery today*, 2018.
- [65] Rafael Gómez-Bombarelli, Jorge Aguilera-Iparraguirre, Timothy D Hirzel, David Duvenaud, Dougal Maclaurin, Martin A Blood-Forsythe, Hyun Sik Chae, Markus Einzinger, Dong-Gwang Ha, Tony Wu, et al. Design of efficient molecular organic light-emitting diodes by a high-throughput virtual screening and experimental approach. *Nature materials*, 15(10):1120–1127, 2016.
- [66] Vishwesh Venkatraman, Sigvart Evjen, and Kallidanthiyil Chellappan Lethesh. The ionic liquid property explorer: An extensive library of task-specific solvents. *Data*, 4(2):88, 2019.
- [67] Peter Bjørn Jørgensen, Murat Mesta, Suranjan Shil, Juan Maria García Lastra, Karsten Wedel Jacobsen, Kristian Sommer Thygesen, and Mikkel N Schmidt. Machine learning-based screening of complex molecules for polymer solar cells. *The Journal of chemical physics*, 148(24):241735, 2018.
- [68] Daniel C Elton, Zois Boukouvalas, Mark S Butrico, Mark D Fuge, and Peter W Chung. Applying machine learning techniques to predict the properties of energetic materials. *Scientific reports*, 8(1):1–12, 2018.
- [69] Wouter Kool, Herke van Hoof, and Max Welling. Attention, learn to solve routing problems! In *International Conference on Learning Representations*, 2019. URL <https://openreview.net/forum?id=ByxBFsRqYm>.
- [70] Diederik P Kingma and Jimmy Ba. Adam: A method for stochastic optimization. *arXiv preprint arXiv:1412.6980*, 2014.
- [71] Stephen Walter Gabrielson. Scifinder. *Journal of the Medical Library Association: JMLA*, 106(4):588, 2018.
- [72] David S Wishart, Yannick D Feunang, An C Guo, Elvis J Lo, Ana Marcu, Jason R Grant, Tanvir Sajed, Daniel Johnson, Carin Li, Zinat Sayeeda, et al. Drugbank 5.0: a major update to the drugbank database for 2018. *Nucleic acids research*, 46(D1):D1074–D1082, 2018.

A Implementation details of the genetic operators

In this paper, we use crossover and mutation proposed by Jensen [22] for exploring the chemical space.

Crossover The crossover randomly applies either `non_ring_crossover` or `ring_crossover`, with equal probability. This generates two (possibly invalid) child molecules. If both the child molecules are invalid, e.g., violating the valency rules, the crossover is re-applied with limited number of trials. If valid molecules exist, then we choose one of them randomly. In the following, we provide further details on the `non_ring_crossover` and `ring_crossover`.

- a. The `non_ring_crossover` cuts an arbitrary edge, which does not belong to ring, of two parent molecules, and then attach the subgraphs from different parent molecules.
- b. The `ring_crossover` cuts two edges in an arbitrary ring, and attach the subgraphs from different parent molecules.

Mutation The mutation randomly applies one of the seven different ways for modifying a molecule: `atom_deletion`, `atom_addition`, `atom_insertion`, `atom_type_change`, `ring_bond_deletion`, `ring_bond_addition`, and `bond_order_change`. After mutation, if the modified molecule is not valid, we discard it and re-apply mutation. Details of seven different ways of modifying a molecule are as follows.

- a. The `atom_deletion` removes a single atom and rearrange neighbor molecules with minimal deformation from the original molecule.
- b. The `atom_addition` connects a new atom to a single atom.
- c. The `atom_insertion` puts an atom between two atoms.
- d. The `atom_type_change` newly changes a type of an atom.
- e. The `bond_order_change` alters the type of a bond.
- f. The `ring_bond_deletion` cuts a bond from ring.
- g. The `ring_bond_addition` creates a "shortcut" between two connected atoms.

B Additional experiments

Table 3: Experiment results for quantitative estimate of drug-likeness (QED) task.

Algorithm	Type	Objective
MCTS ^[Jensen 2019]	MCTS	0.851
ORGAN ^[Guimaraes et al. 2017]	DRL	0.896
JT-VAE ^[Jin et al. 2018]	DEO	0.925
ChemGE ^[Yoshikawa et al. 2018]	GA	0.948
GCPN ^[You et al. 2018]	DRL	0.948
MRNN ^[Popova et al. 2019]	DRL	0.948
MolDQN ^[Zhou et al. 2019]	DRL	0.948
GraphAF ^[Shi et al. 2020]	DRL	0.948
GB-GA ^[Jensen 2019]	GA	0.948
HC-MLE ^[Jensen 2019]	DRL	0.948
MSO ^[Winter et al. 2019]	DEO	0.948
GEGL [†] (Ours)	DRL	0.948

Table 4: Experimental results on relatively straight-forward tasks from the Guacamol benchmark.

Task	ChEMBL ^[56]	MCTS ^[22]	ChemGE ^[21]	HC-MLE ^[13]	GB-GA ^[22]	GEGL ^(Ours)
logP (target: -1.0)	1.000	1.000	1.000	1.000	1.000	1.000
logP (target: 8.0)	1.000	1.000	1.000	1.000	1.000	1.000
TPSA (target: 150.0)	1.000	1.000	1.000	1.000	1.000	1.000
CNS MPO	1.000	1.000	1.000	1.000	1.000	1.000
C ₇ H ₈ N ₂ O ₂	0.972	0.851	0.992	1.000	0.993	1.000
Pioglitazone MPO	0.982	0.941	1.000	0.993	0.998	0.999

In this section, we provide additional experimental results for the tasks in the GuacaMol benchmark Brown et al. [28] that were determined to be relatively more straight-forward than other tasks. To this end, we first report our result for unconstrained optimization of the quantitative estimate of drug-likeness (QED) [49] in Table 3. Next, we evaluate GEGL on other tasks from the GuacaMol benchmark in Table 4. In the Table 3 and 4, we observe GEGL to achieve the highest scores for six out of seven tasks. See Appendix F for details on the tasks considered in this section.

C Training details

In this section, we provide the implementation details for our experiments.

Hardware. All of the experiments were processed using single GPU (NVIDIA RTX 2080Ti) and eight instances from a virtual CPU system (Intel Xeon E5-2630 v4).

Common details for GEGL. For all experiments, we use priority queue of fixed size $K = 1024$. At each step, we sample 8192 molecules from the apprentice and the expert policy to update the respective priority queues. Adam optimizer [70] with learning rate of 0.001 was used to optimize the neural network with a mini-batch of size 256. Gradients were “clipped” by a norm of 1.0.

The apprentice policy is constructed using three-layered LSTM associated with hidden state of 1024 dimensions and dropout probability of 0.2. At each step of GEGL, the apprentice policy generates 8192 molecules. Among the 8192 samples, *invalid* molecules, e.g., molecules violating the valency rules, are filtered out from output of the apprentice policy.

The expert policy generates a molecule by selecting 8192 pair of molecules to apply crossover. Then for each valid molecules generated, mutation is applied with probability of 0.01. Similar to the apprentice policy, invalid molecules are filtered out from output of the expert policy.

Optimization-specific details for GEGL For the unconstrained optimization of PenalizedLogP, i.e., Table 1a, we pretrain the apprentice policy on the ZINC dataset [54] for 10 epochs (over the whole dataset). Next, we run GEGL for 200 steps. For this experiment, we constrain the maximum length of SMILES to be 81 (following Jensen [22], Nigam et al. [23], and Yang et al. [50]).

For the similarity-constrained optimization of PenalizedLogP, i.e., Table 1b, we again pretrain the apprentice policy on the ZINC dataset [54] for 10 epochs (over the whole dataset). Using the pretrained network, we run GEGL for 50 steps, for each reference molecule x_{ref} from the 800 low-scoring molecules. Furthermore, we initialize the apprentice’s priority queue \mathcal{Q} with the reference molecule x_{ref} , i.e., $\mathcal{Q} \leftarrow \{x_{\text{ref}}\}$. For this experiment, we constrain the maximum length of SMILES to be 100.

For the Gaucamol benchmark, i.e., Table 2 and 4, we use the network provided by Brown et al. [28],⁶ that was pretrained on the ChEMBLE [56] dataset. For each tasks, we run GEGL for 200 steps. For this experiment, we constrain the maximum length of SMILES to be 100.

Details for baselines. All of the reported results are reported by the existing works, with the exception of GraphAF [18] in Table 1b and baselines in Table 2b. To be specific, we re-evaluate the molecules generated from GraphAF using “our” implementation of PenalizedLogP (See Appendix E).⁷ For Table 2b, we run the implementation provided by Brown et al. [28].⁶

⁶https://github.com/BenevolentAI/guacamol_baselines

⁷This leads to a sub-optimal performance, since we use the GraphAF model trained under a different implementation of PenalizedLogP; we provide a fair comparison in Table 5b.

D Baselines for de novo molecular design

In this section, we briefly describe the algorithms we used as baselines for evaluating our algorithm.

1. GVAE+BO [7] trains a *grammar* variational autoencoder and applies Bayesian optimization on its embedding space.
2. SD-VAE [11] propose a *syntax directed* variational autoencoder and applies Bayesian optimization on its embedding space.
3. ORGAN [6] trains a generative adversarial network along with reinforcement learning for maximizing the object.
4. VAE+CBO [19] trains a molecule-generating variational autoencoder and applies constrained Bayesian optimization on its embedding space.
5. CVAE+BO [8] trains a *constrained* variational autoencoder and applies Bayesian optimization on its embedding space.
6. JT-VAE [12] trains a *junction tree* variational autoencoder and applies Bayesian optimization on its embedding space.
7. ChemTS [50] proposes a SMILES-based genetic algorithm.
8. GCPN [9] trains a policy parameterized with graph convolutional network with reinforcement learning to generate highly-rewarding molecules. The reward is defined as a linear combination of the desired property of the molecule and a discriminator term for generating "realistic" molecules.
9. Molecular recurrent neural network (MRNN) [15] trains a recurrent neural network using reinforcement learning.
10. MolDQN [17] trains a molecular fingerprint-based policy with reinforcement learning.
11. GraphAF [18] trains a auto-regressive flow model with reinforcement learning.
12. GB-GA [22] proposes a graph-based genetic algorithm.
12. MCTS [22] proposes a Monte Carlo tree search algorithm.
13. MSO [16] applies particle swarm optimization on the embedding space of a variational autoencoder.
14. DEFactor [14] trains a variational autoencoder where computational efficiency was enhanced with differentiable edge variables.
15. VJTNN [51] trains a graph-to-graph model with supervised learning on the highly-rewarding set of molecules.
16. HC-MLE [13] proposes a "hill-climbing" variant of reinforcement learning to train a recurrent network.
17. CReM [39] proposes a genetic algorithm based on "chemically reasonable" genetic operator to generate a set of chemically reasonable molecules.
18. HierG2G [20] trains a graph-to-graph, hierarchical generative model with supervised learning on the highly-rewarding set of molecules.
19. DA-GA [23] proposes a genetic algorithm based on its fitness function augmented with a discriminator which assigns higher scores to "novel" elements.

E Two ways of computing the PenalizedLogP score

Table 5: Experimental results on the optimization of PenalizedLogP with similarity constraint of δ , based on evaluating RingPenalty using AtomRings (a) and cycle_basis (b) functions from Python’s NetworkX and RDKit packages, respectively. †We report the average and standard deviation of the objectives collected over 800 molecules.

(a) Evaluation using AtomRings				(b) Evaluation using cycle_basis			
δ	Algorithm	Objective	Succ. rate	δ	Algorithm	Objective	Succ. rate
0.4	MolDQN [Zhou et al. 2019]	3.37 \pm 1.62	1.00	0.4	JT-VAE [Jin et al. 2018]	0.84 \pm 1.45	0.84
	DA-GA [Nigam et al. 2020]	5.93 \pm 1.41	1.00		GCPN [You et al. 2018]	2.49 \pm 1.30	1.00
	GEGL† (Ours)	7.37 \pm 1.22	1.00		VJTNN [Jin et al. 2019]	3.55 \pm 1.67	-
0.6	MolDQN [Zhou et al. 2019]	1.85 \pm 1.21	1.00	0.6	GraphAF [Shi et al. 2020]	8.21 \pm 6.51	1.00
	DA-GA [Nigam et al. 2020]	3.44 \pm 1.09	1.00		GEGL† (Ours)	15.00 \pm 6.74	1.00
	GEGL† (Ours)	3.98 \pm 1.22	1.00		JT-VAE [Jin et al. 2018]	0.21 \pm 0.71	0.47
				GCPN [You et al. 2018]	0.79 \pm 0.63	1.00	
				VJTNN [Jin et al. 2019]	2.33 \pm 1.17	-	
				GraphAF [Shi et al. 2020]	4.98 \pm 6.49	0.97	
				GEGL† (Ours)	9.69 \pm 6.00	0.99	

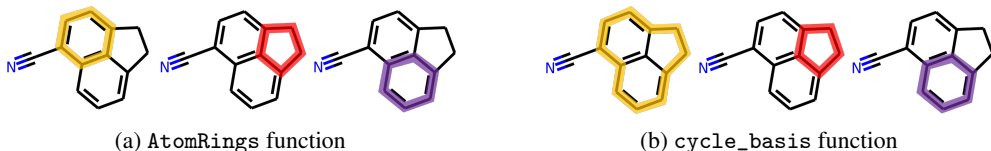


Figure 7: Illustration for the set of cycles obtained from AtomRings and cycle_basis functions applied to the molecule N#CC1=CC=C2CCC3=C2C1=CC=C3 in the ZINC dataset.

In this section, we describe how the PenalizedLogP score is measured in two different ways in the literature. First, recall the following definition of PenalizedLogP score:

$$\text{PenalizedLogP}(x) = \text{LogP}(x) - \text{SyntheticAccessibility}(x) - \text{RingPenalty}(x).$$

Existing works differ on the way of obtaining the list of atom rings for computing RingPenalty, i.e., the penalty for atom rings of size larger than 6. When inspecting the official implementations, we find out that Jin et al. [12],⁸ You et al. [9],⁹ Jin et al. [51],¹⁰ and Shi et al. [18]¹¹ obtain the list of rings from the cycle_basis function in the Python’s NetworkX library.¹² In contrast, Zhou et al. [17]¹³, Nigam et al. [23]¹⁴, and our work use the AtomRings function from the Python’s RDKit library¹⁵ to obtain the list of rings.

This results in a slightly different PenalizedLogP scoring for the same molecule. To be specific, the cycle_basis function extracts an “arbitrary” set of simple cycles which forms a basis for cycle space of the molecular graph. In contrast, the AtomRings function aims at extracting a “small set of smallest rings” describing the whole molecule.¹⁶ We also provide an example in Figure 7 where two functions produce a different list for a same molecule. Here, we observe that PenalizedLogP defined with respect to the cycle_basis function penalizes the molecule, while AtomRings function does not.

⁸<https://github.com/wengong-jin/icml18-jttnn>

⁹https://github.com/bowenliu16/rl_graph_generation

¹⁰<https://github.com/wengong-jin/iclr19-graph2graph>

¹¹<https://openreview.net/forum?id=S1esMkHYPr>

¹²<https://networkx.github.io/>

¹³https://github.com/google-research/google-research/tree/master/mol_dqn

¹⁴<https://github.com/aspuru-guzik-group/GA>

¹⁵<https://github.com/rdkit/rdkit>

¹⁶https://www.rdkit.org/docs/RDKit_Book.html

We consider the `AtomRings` function to be more aligned with the definition of “atom rings” than the `cycle_basis` function. Our choice mainly comes from the fact that the `AtomRings` is defined more consistently and defined specifically for capturing the atom rings in the molecule. Hence, we evaluate `PenalizedLogP` using the `AtomRings` function in Section 4.1. Note that we only re-evaluate GraphAF [18] in Table 1, since GraphAF was the best-performing baseline with different criteria for computing the `PenalizedLogP` score (See Appendix C for how we re-evaluate GraphAF).

For completeness, in Table 5, we re-evaluate GEGL for Table 1b using both the `AtomRings` and the `cycle_basis` functions with the corresponding baselines.¹⁷ Here, we observe that GEGL outperform the baselines regardless of the choice for `PenalizedLogP` score. Especially, GEGL achieves a higher score even when computing `PenalizedLogP` with the `cycle_basis` function. This is because the scores for the reference molecules are much lower when computing for this case; the `cycle_basis` function tends to capture larger cycles in the molecules and get larger penalty. Finally, we remark that that we do not re-evaluate Table 1a since the generated molecules (for unconstrained optimization of `PenalizedLogP`) do not contain cycles and the evaluated results do not change even when switching to `cycle_basis` function.

¹⁷Note that the 800 lowest-scoring molecules are determined accordingly for each criteria of `PenalizedLogP`.

F Details on the GuacaMol benchmark

Given a set of molecules $\mathcal{X} = \{\mathbf{x}_s\}_{s=1}^{|\mathcal{X}|}$ and a set of positive integers \mathcal{S} , tasks in the GuacaMol benchmark evaluate their score as follows:

$$\text{GuacaMolScore}(\mathcal{X}) := \sum_{S \in \mathcal{S}} \sum_{s=1}^S \frac{r(\mathbf{x}_{\Pi(s)})}{S|\mathcal{S}|}, \text{ where } r(\mathbf{x}_{\Pi(s)}) \geq r(\mathbf{x}_{\Pi(s+1)}) \text{ for } s = 1, \dots, |\mathcal{X}|-1,$$

where r is the task-specific molecule-wise score and Π denotes a permutation that sorts the set of molecules \mathcal{X} in descending order of their metrics.

Next, we further provide details on the tasks considered in the GuacaMol benchmark.

- **Rediscovery.** The {celecoxib, troglitazone, thiothixene} rediscovery tasks desire the molecules to be as similar as possible to the target molecules. The algorithms achieve the maximum score when they produce a molecule identical to the target molecule. These benchmarks have been studied by Zaliani et al. [57] and Segler et al. [45].
- **Similarity.** The {aripiprazole, albuterol, mestranol} similarity tasks also aim at finding a molecule similar to the target molecule. It is different from the rediscovery task since the metric is evaluated over multiple molecules. This similarity metric has been studied by Willett et al. [58].
- **Isometry.** The tasks of $C_{11}H_{24}$, $C_9H_{10}N_2O_2PF_2Cl$, $C_7H_8N_2O_2$ attempt to find molecules with the target formula. The algorithms achieve an optimal score when they find all of the possible isometric molecules for the tasks.
- **Median molecules.** The median molecule tasks searches for molecules that are simultaneously similar to a pair of molecules. This previously has been studied by Brown et al. [38].
- **Multi property optimization.** The {osimertinib, fexofenadine, ranolazine, perindopril, amlodipine, CNS, Pioglitazone} multi property optimization (MPO) tasks attempt to fine-tune the structural and physicochemical properties of known drug molecules. For example, for the sitagliptin MPO benchmark, the models must generate molecules that are as dissimilar to sitagliptin as possible, while keeping some of its properties.
- **Other tasks.** The valsartan SMARTS benchmark targets molecules containing a SMARTS pattern related to valsartan while being characterized by physicochemical properties corresponding to the sitagliptin molecule. Next, the scaffold Hop and decorator Hop benchmarks aim to maximize the similarity to a SMILES strings, while keeping or excluding specific SMARTS patterns, mimicking the tasks of changing the scaffold of a compound while keeping specific substituents, and keeping a scaffold fixed while changing the substitution pattern. The LogP tasks aim at generating molecules with the targeted value of octanol-water partition coefficient. The TPSA task attempts to find a molecule with the targeted value of topological polar surface area. The QED task aims at maximizing the quantitative estimate of drug-likeness score.

G Discussion on GuacaMol molecules

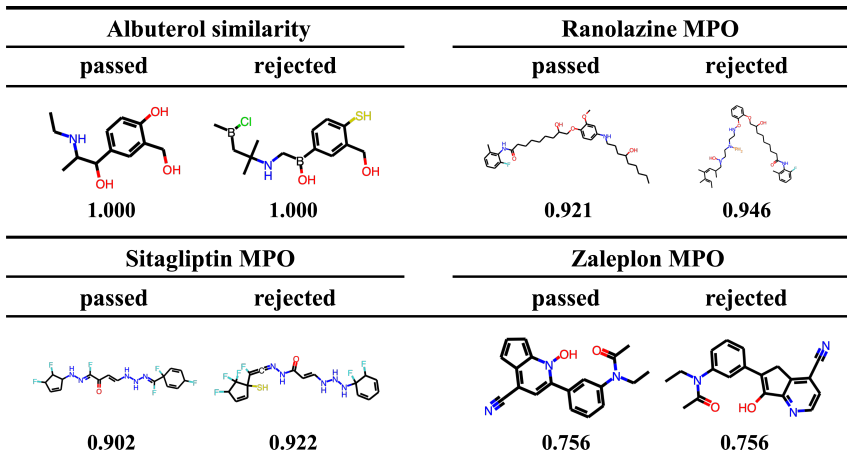


Figure 8: Illustration of the molecules generated for the GuacaMol benchmark, that have passed and rejected from the filtering procedure. Below each molecule, we also denote the associated objectives.

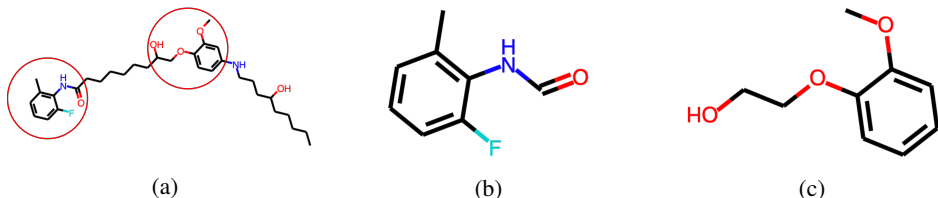


Figure 9: (a) The main fragments in the passed molecule of Ranolazine MPO are marked. Two main fragments exist in reality: (b) N-(2-fluoro-6-methylphenyl) formamide, (c) 2-(2-methoxyphenoxy) ethanol.

In this section, we further provide descriptions on the molecules generated from GEGL for the tasks of GuacaMol benchmark, illustrated in Figure 8.

Molecules passed from the post-foc filtering. We first report some of the discovered molecules that pass the post-hoc filtering procedure and have realistic yet novel structures. For example, one may argue that the passed molecule for the Ranolazine MPO (in Figure 8) is chemically realistic; its main fragments of N-(2-fluoro-6-methylphenyl) formamide, (Figure 9b) and 2-(2-methoxyphenoxy) ethanol (Figure 9c) actually exist in reality. We have also verified the molecule to be novel from the chemical databases such as Scifinder [71] and Drugbank [72]. We provide the detailed illustration for the discovered molecule in Figure 9.

Molecules rejected from the post-foc filtering. In Figure 8, we illustrate an example of rejected molecules for the Albuterol similarity, Ranolazine MPO, Sitagliptin MPO, and Zaleplon MPO, respectively. They are filtered out as they are chemically reactive with high probability. Specifically, the molecule from the Albuterol similarity was rejected due to containing a SMILES of SH, i.e., *15 Thiols*. The molecule from the Ranolazine MPO was due to $C=CC=C$ ¹⁸, and that from the Sitagliptin MPO was due to $NNC=O$, i.e., *acylhydrazide*. Functional groups like SH, $C=CC=C$, and $NNC=O$ are known to be reactive with high probability, hence they are rejected from the filtering procedure.

¹⁸Note that $C=CC=C$ in a ring is stable, but $C=CC=C$ not in a ring is reactive, i.e., the left side of the molecule.